Theor Chem Acc (2011) 128:713–725
DOI 10.1007/s00214-010-0815-6

REGULAR ARTICLE

Understanding the differences in photochemical properties of substituted aminopyrimidines

Mireia Segado · Maria-Angels Carvajal · Isabel Gómez · Mar Reguero

Received: 16 July 2010 / Accepted: 6 September 2010 / Published online: 26 September 2010

Abstract The luminescent patterns of several members of the aminopyrimidine family are very different, showing not fluorescence at all, only a fluorescence band, normal or anomalous, or dual fluorescence, depending on the substituents and on the environment (gas phase vs. polar solvents). In this work, we study the lowest excited states of several members of this family that exhibit different fluorescence patterns to try to explain their photochemistry and to understand the effect of the substituents and the environment. We have found that several excited states (local excited (LE), charge transfer (CT) and n_N–π^* states) have minima on the lowest excited potential energy surface (S_1), being their relative energy the determinant factor of the luminescent behavior. If the more stable S_1 minima are of n_N–π^* character, a non-radiative deexcitation channel is the most efficient and the system shows no fluorescence. If the CT and/or LE states are the most stable, the non-radiative deactivation channel is not accessible and the system fluoresces. The relative energies of the CT and LE minima (affected by substituents and by the presence of a polar solvent) and the different magnitude of the oscillator strength for the radiative transition to the ground state determine which emission is more efficient, giving place to normal, anomalous or dual fluorescence. The study has been carried out by CASSCF/CASPT2 computations, including the solvent effect by means of the PCM model.

Keywords Photochemistry · Intramolecular charge transfer · Fluorescence · Aminopyrimidines · Ab initio calculations

1 Introduction

Aminopyrimidines are molecules of increasing interest because of their important role as underlying constituents of several nucleobases (cytosine, uracyl and thymine) and its presence in a large number of natural products [1] such as vitamin B1 [2]. They show interesting photochemical properties and likely play an important role in some of the photochemical processes undergone by DNA. Besides constituting one of the most important molecules for living organisms, amino-substituted pyrimidines are also present in agrochemicals [3], in pharmaceutical agents [4] and in material science [5–9].

Due to the substitution of one or several pyrimidine hydrogens by amino or functionalized amino groups, aminopyrimidines are susceptible to undergo intramolecular charge transfer processes (ICT), because of the ability of the amino group to act as electron donor and to the acceptor character of the aromatic heterocycle. Since these two moieties are linked by a single bond, the state with charge separation can be favored by rotation of the donor and the acceptor moieties and be further stabilized by an appropriate environment like a polar solvent (Scheme 1) [10–14]. If the CT species is stable enough, it can undergo radiative deactivation and produce an anomalous fluorescence band. The competition between the species responsible for the normal fluorescence, usually called locally

Published as part of the special issue celebrating theoretical and computational chemistry in Spain.

Electronic supplementary material The online version of this article (doi:10.1007/s00214-010-0815-6) contains supplementary material, which is available to authorized users.

M. Segado · M.-A. Carvajal · I. Gómez · M. Reguero (✉)
Departament de Química Física i Inorgánica, Facultat de Química, Universitat Rovira i Virgili, Campus Sescelades, Marcel.lí Domingo, 43007 Tarragona, Spain
e-mail: mar.reguero@urv.net

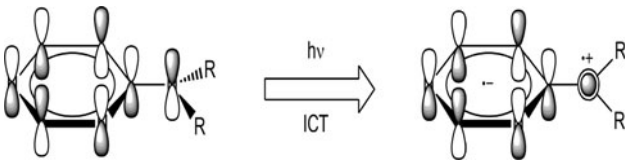

Scheme 1 Twisted intramolecular CT mechanism

excited (LE), and the CT gives raise to different luminescence patterns. Hence, depending on structural or environmental factors, the fluorescence spectrum can show only the normal fluorescence band, the red-shifted anomalous band, or both, then taking place the so-called dual fluorescence.

For this reason, nature and position of the substituents affect the photochemical properties of the aminopyrimidines. For instance, whereas 4-aminopyrimidine (APD) does not exhibit any fluorescence even in highly polar aprotic solvents, 4-dimethylaminopyrimidine (DMAPD) shows only the normal fluorescence band in gas phase as well as in polar solvents. On the other hand, the 5-methyl-substituted molecules 4-dimethylamino-5-methylpyrimidine (DMA5MPD) and 4-diethylamino-5-methylpyrimidine (DEA5MPD) (Scheme 2) present normal fluorescence in gas phase and only anomalous fluorescence in polar aprotic solvents. Intriguingly, 4-diethylaminopyrimidine (DEAPD) shows only the normal band in gas phase, but dual fluorescence in highly polar aprotic solvents. These results have been explained qualitatively by the twisted intramolecular CT (TICT) model and steric interactions between the substituents, although the reason for the different behavior between DMAPD and DEAPD is still obscure [15, 16].

In spite of the interesting properties of this kind of molecules, for some time they have not attracted much attention, probably because main efforts have been directed towards the aminobenzonitrile family of compounds (DMABN), which present a very promising solvent-dependent fluorescence [17, 18]. However, more recently, the discovering of the several possible deactivation pathways for adenine has renewed the interest in aminopyrimidines, and some theoretical studies have already addressed the deactivation pathways of aminopyrimidine [19, 20]. In the adenine case, the deactivation has been proposed to take place via out-of-plane ring deformation or by means of specific bond-breaking processes but, according to energetic considerations, deactivation must occur through out-of-plane deformations. Concerning aminopyrimidine, recent studies pointed out the existence of $^1(\pi\text{–}\pi^*)$ and $^1(n\text{–}\pi^*)$ and additional states that play a role in their deactivation pathways. Specifically, the latest studies carried out by Barbatti and collaborators show that deactivation of the initially populated S_1 $^1(n\text{–}\pi^*)$ state can go through six possible channels starting from two different $^1(n\text{–}\pi^*)$ minima and proceeding by three minima on the crossing seam of $^1(\pi\text{–}\pi^*)/S_0$ character. This implies a change of character during the deactivation before reaching the ground state. For all the explored reaction pathways, the barrier to overcome is approximately 0.5 eV, except for the path involving relaxation to a planar state, whose barrier is only 0.28 eV and after which the system can reach a C_6-puckered minimum (according to the atom numbering used in this paper, see Scheme 2) on the crossing seam, allowing then an ultrafast deactivation to take place [19, 20].

The aim of the present work is to understand in detail the photochemistry of the aminopyrimidines, studing the ICT mechanism and the competitive photodeactivation pathways to rationalize the effect of the substituents in the photochemical properties of this family of molecules. In order to do so, we have first carried out a complete study of the photochemistry of the prototype molecule APD, and in a second stage, the effect of the substituents has been analyzed by means of a study on the derivatives DMAPD and DMA5MPD in gas phase and in a polar solvent. Finally, some calculations have been performed in the DEAPD derivative to explain its intriguing luminescent behavior. Essential information has been also obtained regarding the nature of the excited states and of the species localized on the potential energy surface of the first excited state.

2 Computational details

The ground state and the six lower singlet excited states for APD, DMAPD, DMA5MPD and DEAP have been studied by means of multiconfigurational self-consistent-field (MCSCF) calculations within the complete active space (CAS) SCF approach. The basis set employed was the double zeta plus polarization 6-31G* basis set [21] for all

Scheme 2 Structure of some aminopyrimidine derivatives: APD, DMAPD, DMA5MPD and DEAPD. Atom labeling is shown for APD

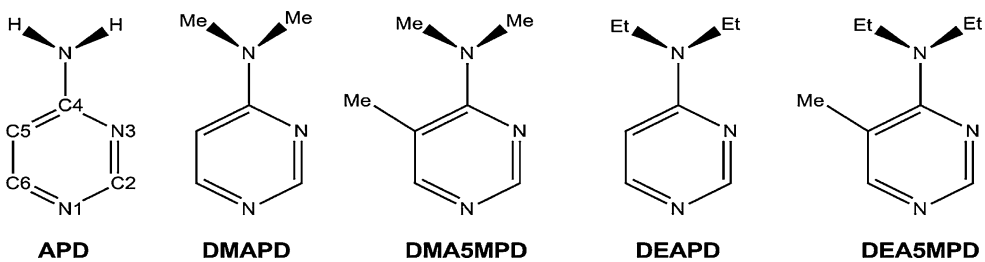

the atoms. All the calculations were carried out by using MOLCAS 7.0 [22] and Gaussian03 [23] suite of programs.

Full geometry optimizations were performed without any symmetry constraint, and numerical frequency calculations were run to determine the nature of the stationary points at the CASSCF level. Conical intersections (CIs) were optimized by using state-averaged orbitals without including the orbital rotation derivative correction to the gradient, which is usually small. This technique finds the lowest energy point on the crossing seam. In this point, the gradient difference and the derivative coupling vectors (branching space) are the coordinates leaving the degeneracy, while the remaining 3 N-8 coordinates (intersection space) preserve the degeneracy, which persists over a wide range of molecular geometries. Although the maximum probability of crossing occurs at the minimum energy point on the intersection, the decay can take place away from that point, depending on the kinetic energy of the system.

In order to obtain a better estimate of the energy of the stationary points found, in a second step, a seven-state SA-CASSCF wave function was used as the reference in the single-state CASPT2 (SS-CASPT2) treatment, and the coupling among the SS-CASTP2 states via dynamic correlation was taken into account through the multi-state CASPT2 (MS-CASPT2) treatment. Hence, the energies presented and discussed along the paper are calculated at the MS-CASPT2 level, unless otherwise stated. The imaginary level shift technique was used to prevent intruder states from appearing, and a shift parameter of 0.3 au was selected after testing. An effective Hamiltonian matrix was constructed in which the diagonal elements correspond to the SS-CASPT2 energies and the off-diagonal terms introduce the coupling to second order of the dynamic correlation energy. In this way, the resulting perturbation-modified CAS (PM-CAS-CI) wave functions were also obtained.

The effect of the dynamic correlation in the energy is not the same for all the excited states considered. This fact can be observed, for instance, in the results reported in Table 1, where the magnitude of the energy difference between states changes substantially when calculated at the CASSCF or at the MS-CASPT2 level. This affects mainly to the optimization of CI's involving states of different nature that have therefore a different energy contribution of the dynamical correlation effect [24, 25]. In this case, the CI optimization becomes a highly non-trivial task, since the standard procedure is to locate the minimum energy point of degeneracy at the CASSCF level. When the energies of the states involved in the CI located are recalculated at the MS-CASPT2 level, the states can become non-degenerate, and in some cases, the energy difference can be quite large. Given that the cost of the CI optimization at the MS-CASPT2 level is not computationally affordable as a routine procedure, to estimate the position and energy of the crossing when the CASSCF description is not accurate enough, linear interpolated internal reaction coordinate (LIIRC) paths are calculated at the MS-CASPT2 level between the minima of the states that cross, to get the profiles of the states of interest along this path.

The CAS employed in these calculations consists of 12 electrons and 11 orbitals, which include the seven orbitals of the aminopyrimidine π system, the two N lone pairs of the in-ring N atoms (n_N) and two additional diffuse n_N pair type orbitals (see Scheme 3). These two n_N orbitals were included in the CAS after analysis of the state average molecular orbitals and the contribution of the configuration state functions (CSF) obtained at CASSCF/MS-CASPT2 level with the smaller CAS(12,9) for the ground state

Table 1 CASSCF(12,11), SS-CASPT2(12,11) and MS-CASPT2(12,11) vertical excitation energies (in kcal mol^{-1}) for the six lowest singlet excited states of APD and corresponding oscillator strength

State	CASSCF		SS-CASPT2		MS-CASPT2		Dipole	Oscillator strength
	Char.	ΔE	Char.	ΔE	Char.	ΔE		
S_1	LE	124.02	NA1	117.21	NA1	116.53	1.75	0.0043
S_2	NA1	133.19	LE	121.35	LE	122.34	3.17	0.0141
S_3	NA2	138.57	NA2	123.05	NA2	124.74	1.89	0.0097
S_4	NS1	168.76	CT	144.74	CT	146.89	5.68	0.1900
S_5	CT	173.92	NS1	150.34	NS1	151.46	1.58	0.0045
S_6	NS2	176.81	NS2	157.78	NS2	159.56	2.50	0.0043

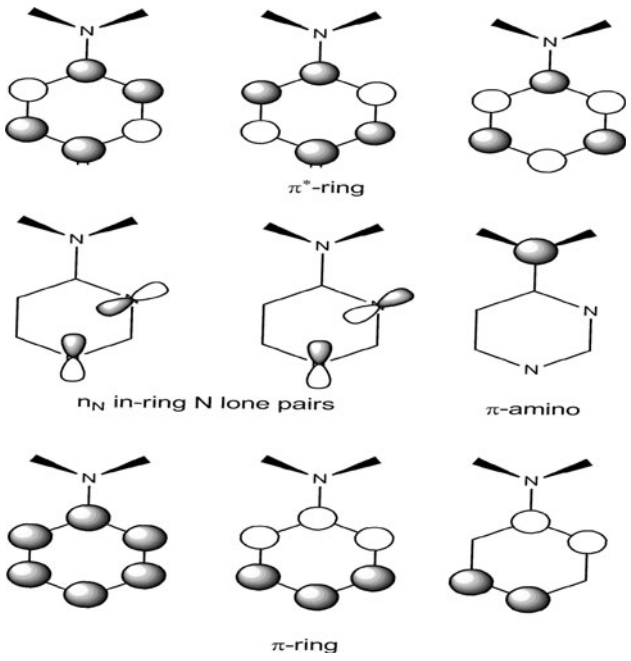

Scheme 3 Schematic representation of the orbitals included in the CAS(12,9). The two additional orbitals included in the CAS(12,11) are virtual orbitals of the n_N in-ring N lone pairs type

minimum and the lower singlet states in the Franck–Condon region. This analysis shows an important mixing at the MS-CASPT2 level between the states involving the N lone pair orbitals (n_N). The strategy of increasing the CAS size to (12,11) allows the correlation associated with such lone pairs to be included already at the CASSCF level, and consequently the obtained energies are more accurate and the mixing between states is removed, so the physical analysis of the results becomes clearer [24–26].

The CAS state interaction (CASSI) protocol and the PM-CAS-CI functions were used to compute transition dipole moments and oscillator strengths, which are proportional to the transition probability for absorption and radiative emission.

To take into account the solvent effects in the photochemistry of the APD derivatives, the reaction field formalism was used and a polarizable continuum model (PCM) [27–29] was employed. The solvent parameters correspond to acetonitrile, to try to reproduce the usual experimental conditions, and the size of the tesserae of the solute cavity were set to 0.4. Since the object of study is the emission of S_1 intermediates, the second root is used to generate the solvation charges, which will perturb the rest of the states considered.

In the presentation of the results and discussion of the physical nature of the states, only the configurations that contribute most to the result are taken into account. However, the data was generated using all the possible configurations, necessary to get an accurate description of the states.

3 Results and discussion

3.1 Unsubstituted aminopyrimidine, APD

First of all, vertical excitations at the optimized geometry of the ground state of the parent system were computed. The character of the lowest excitations is displayed in Scheme 4, and the results for the energies and oscillator

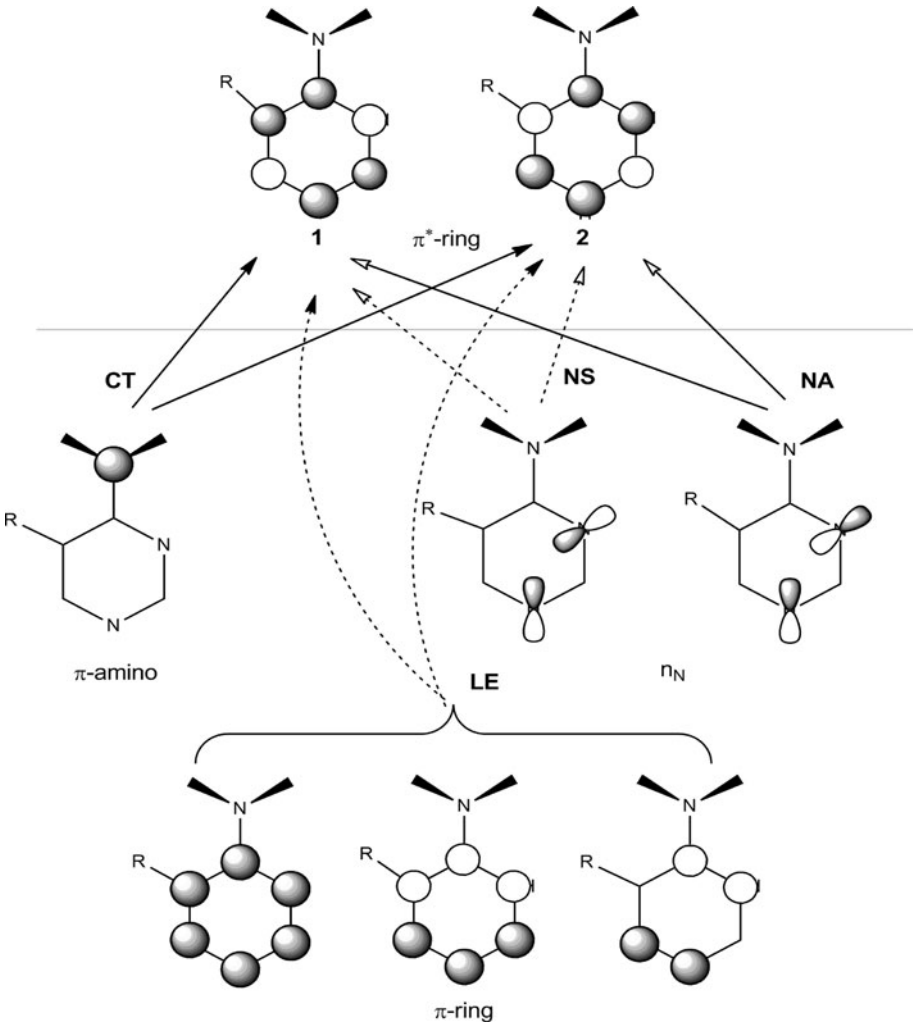

Scheme 4 Schematic representation of the lowest excitations of APD. The *gray line* separates the occupied orbitals (below the line) from the virtual π^* orbitals (labeled *1* and *2*), which are responsible for the main excitations. The type of transition is labeled in *bold* characters: *CT* stands for charge transfer (*solid lines* and *arrows*), *LE* for locally excited (*dashed lines* and *solid arrows*) and *NS* and *NA* for the excitations arising from the two possible combinations (*symmetric* and *antisymmetric*) of the N lone pair orbitals (*hollowed arrows*)

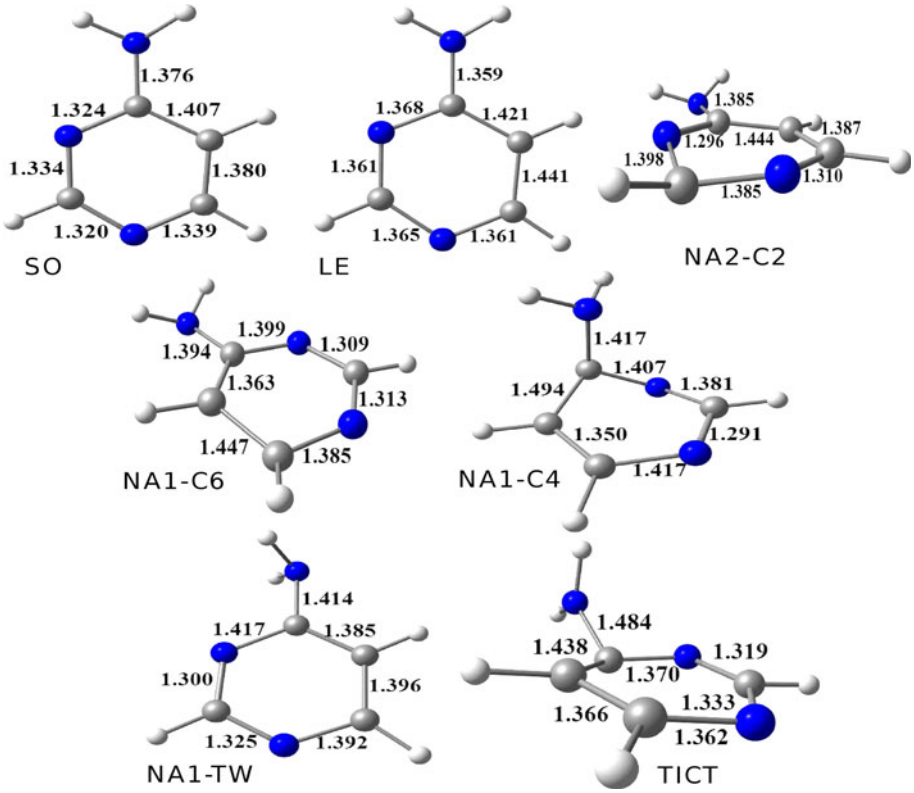

Fig. 1 Optimized structures of S_0 and S_1 APD minima

strengths are shown in Table 1. Several states are characterized: the locally excited LE (excitation in the ring), four states generated by excitations of the n_N in-ring lone pairs to the lowest π^*-ring orbitals, which are labeled NS and NA to indicate excitation from the symmetric (NS) and antisymmetric (NA) combination of n_N orbitals; and finally the charge transfer state (CT), characterized by the transition of an electron from the amino group to the π^*-ring orbitals. While the NS and NA transitions can be qualitatively described as monoexcitations, the LE transition involves depopulation of all three π-ring orbitals of the active space and occupation of the two π^*-ring, although the totally symmetric π-ring orbital undergoes the minor change in its occupation (from 1.96 to 1.88) and the main contribution comes from the other two π-ring orbitals, whose population changes from 1.91 to 1.32 and 1.58 at the CASSCF level. Concerning the CT state, it can be interpreted, in terms of PM-CAS-CI natural orbital occupancies, as a state involving one excitation from the out of ring amino group to the π^*-ring orbitals. MS-CASPT2 results indicate that absorption populates mainly the CT state, that is the fourth excited state, which shows an oscillator strength much larger than that of the rest of the states considered. This result is in good agreement with INDO/S calculations of Herbich for this kind of molecules [15].

As commented in Sect. 2, it is remarkable the significant role of the dynamic correlation in the stabilization of some of the excited states (mainly the CT and both NS), as can be seen by comparing the CASSCF and CASPT2 results.

The next step in this study was to locate and characterize the minima on the S_1 potential energy surface. We located a LE, a CT, a LN1 minima and other three minima of LN2 character (geometries shown in Fig. 1, energies collected in Table 2). The LE minimum is totally planar except for the NH_2 group, which is pyramidalized. It is computed to be 110.27 kcal mol^{-1} above the ground state minimum and has a vertical energy with respect to the ground of 107.5 kcal mol^{-1}. The main contributions to the LE wave function are two CSF involving monoexcitations from the π-ring orbitals 1 and 2 (see Scheme 4), with coefficients 0.76 and 0.33, respectively. The CT minimum lies 116.35 kcal mol^{-1} over the ground state minimum, and its geometry has the characteristics of a twisted ICT state

Table 2 MS-CASPT2 energies relative to the S_0 minimum (ΔE), vertical energies (both in kcal mol^{-1}), dipole moments (in Debye) and oscillator strengths of the characterized S_1 minima for the APD molecule

Minimum	ΔE	Vertical energy	Dipole moment	Oscillator strength
LE	110.3	107.5	3.56	0.0310
NA2	101.9	70.5	1.97	0.0013
NA1–C6	103.9	77.9	1.89	0.0079
NA1–C4	109.5	33.0	3.04	0.0004
NA1–TW	104.5	80.4	0.50	0.0087
TICT	116.3	74.0	7.76	0.0033

(TICT), with the C–NH_2 group pyramidalized and twisted with respect to the ring plane. Analysis of the wave function shows that it consists mainly in an excitation from the π-amino orbital to the π^*-ring 1 orbital. The computed dipole moment of about 5.68 Debye confirms the CT nature of this species. The NA2 minimum is C_2-puckered, since this deformation of the ring stabilizes the excitation from the NA orbital to the π^*-ring 2 orbital, according to the CSF description of the state. It is 101.94 kcal mol^{-1} above the ground state minimum. The three NA1 minima found are associated with excitations from the NA orbital to the π^*-ring 1 orbital: a C_6-puckered minimum in which the amino group stays in the molecular plane (NA1–C6 in Fig. 4), a similar C_4-puckered structure (NA1–C4) and a planar minimum with the amino group pyramidalized and perpendicularly oriented with respect to the ring plane (twisted geometry, NA1–TW). Their energies relative to the ground state minimum are 103.9, 109.5 and 104.5 kcal mol^{-1}, respectively. Although the NA1–C4 lies high in energy, it can be relevant, because the wave function obtained at the MS-CASPT2 level shows an important mixing with the ground state, and a conical intersection can be expected to be quite close to this NA1–C4 minimum. Consequently, if this minimum is populated, the system will easily reach a non-radiative deactivation channel to the ground state. This possibility will be discussed below. On the other hand, the NA1–TW minimum does not seem to have an important role in APD photochemistry, but it can be important for the substituted amynopyrimidines photochemistry, as will also be discussed latter.

The fact that the minima of the excited states are all located on the S_1 surface indicates that there must exist a large number of crossings between the corresponding PES. In such a case, we will have to locate the lowest energy paths connecting the different minima to elucidate which ones can be populated. Nevertheless, we have to know first the evolution of the system immediately after the initial excitation.

To obtain a general picture of these first steps, we had to investigate the evolution of the system in the state populated with the initial excitation, i.e. the CT, from the Franck–Condon geometry. To do so, we obtained a LIIRC path from the Franck–Condon region to the TICT minimum and calculated at the MS-CASPT2 level the profiles of the PES of the first five excited states (Fig. 2). The LIIRC path shows that, following the geometry relaxation path, the CT surface crosses the NA2, NA1 and LE surfaces. It means that there are direct paths to populate all this minima, but the most favored one will be the path leading to the NA2 minima, because this is the first crossing in the CT relaxation path and because this minimum is the most stable one and consequently

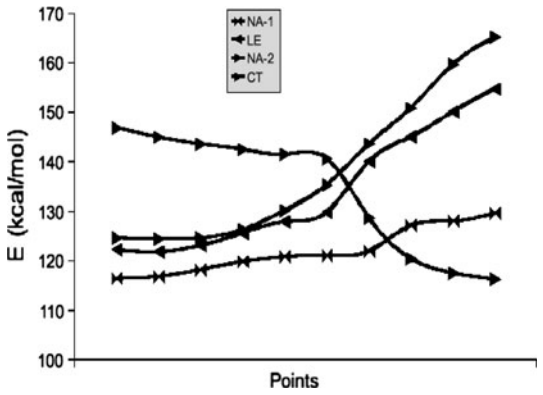

Fig. 2 MS-CASPT2(12,11) LIIRC path from the Franck–Condon region to the TICT minimum. Profiles of the CT, NA2, NA1 and LE state are depicted. S_0 curve is not shown for the sake of clarity

thermodynamically favored. Nevertheless, given the small energy differences between some of the S_1 minima, if the barriers of these paths connecting minima are not too high, their populations will equilibrate along adiabatic paths on the S_1 surface. For this reason, we looked for CI's and TS's on the S_1 PES.

A CI between the NA2 and LE states was found, with a quasi planar ring conformation (see Fig. 3), hence being very close to the Franck–Condon region. It lies only 10.2 and 1.9 kcal mol^{-1} above the NA2 and the LE minima, respectively. Between the NA2 and NA1 states another CI was found. At its minimum energy point, the out-of-ring amino group is slightly more pyrimidalized than at the LE minimum. It is located 8.1 and 6.1 kcal mol^{-1} over the NA2 and NA1–C6 minima. This CI constitutes a low barrier that can be overcome with the excess of excitation energy that the system keeps after the initial absorption. If the NA1–C6 minimum is populated, the system can easily reach the NA1–TW minimum by overcoming an almost negligible barrier of 0.7 kcal mol^{-1}. This transition state involves twisting of the out-of-ring amino group with respect to the benzene plane and planarization of the puckered C_6. In summary, since the energetic barriers connecting the S_1 LE and NA minima are low, all of them can be populated, although the thermodynamic equilibrium favors population of the NA states rather than the LE minimum.

Another set of CIs were found, but these ones connecting the NA states with the ground state. Their low energies, 121.9 for the CI NA2/S_0, 115.7 for the CI NA1–C6/S_0 and 109.0 kcal mol^{-1} for the CI NA1–C4/S_0, make them easily accessible from the minima and consequently open very efficient paths for non-radiative deactivations.

The connection between the CT and LE states is a crucial point in other systems with ICT like the aminobezonitrile family [30, 31]. For this reason and for the sake of comparison, we also investigated this possible reaction

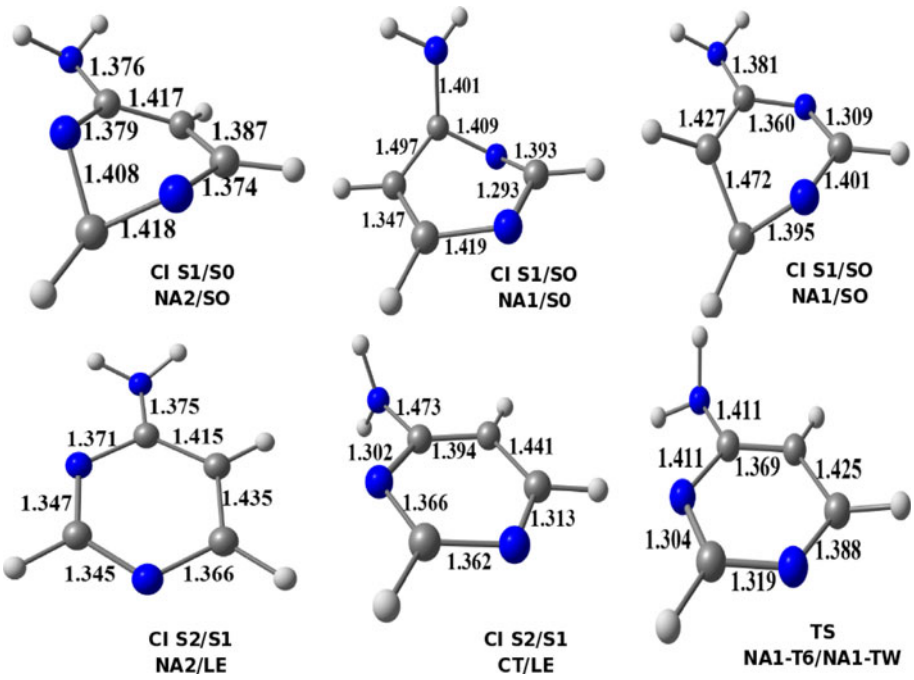

Fig. 3 Optimized TS's and CI's on the S_1 surface of APD

path in APD. For the reasons commented in the Computational details section, though, looking for the lowest energy connection between these states is not an easy task. A minimum energy point of the CI between the LE and CT states was found at CASSCF(8,7) level, high above the LE minimum (34.7 kcal mol^{-1} above). When the energies of both states were recalculated at the MS-CASPT2(12,11) level, though, the LE and CT states were not degenerate any longer (see Online Resource for details), but continued being well above the LE minimum. This result points out that any crossing between the CT and the LE states is not easily accessible.

In conclusion, we predict that the equilibrium between the different minima on the S_1 surface will be displaced favoring the population of the NA minima. From there, the CIs with the ground state are easily accessible, so the non-radiative deactivation is the most efficient channel. Consequently, no luminescence is expected from the APD, nor from the normal band, neither from the anomalous one. This is consistent with the absence of radiative experimental data for this molecule, and finally, it can be related to the high energy of the CT and LE states for the non-substituted APD. As it will be shown below, substituted aminopyrimidines behave very differently.

3.2 Substituted aminopyrimidines DMAPD, DMA5MPD and DEAPD

To study how the substituents affect the luminescence of the members of the aminopyrimidine family, we center our attention in the regions of the PES's that proved to be crucial in the photochemistry of the parent system. That is, we will analyze the relative energies of the states at the Franck–Condon region, the energetics of the most stable S_1 minima and the height of the barriers to equilibrate them in the substituted APDs.

To begin with, the geometry of the ground state minima was optimized for DMAPD, DMA5MPD and DEAPD (Figs. 4, 6, and 8). Bond distances and angles remain nearly the same for all the studied compounds. However, while DMAPD and DEAPD maintain a planar geometry, for the *ortho*-substituted DMA5MPD molecule, the amino group is twisted and C_5 is slightly puckered. This distortion results in a torsion angle of about 39° between the nearest methyl groups belonging to the amino moiety and the ring, which is probably fair enough to lower the steric repulsion between the dimethylamino group and the methyl substituent placed in the *ortho* position. Concerning the pyramidalization of the amino group, it decreases as the donor ability and size of the substituents increase. Pyramidalization has been estimated by the average of the dihedral angles between the substituents of the amino group and the closest adjacent ring atom, and it varies from 23.3° for the non-substituted APD to 13.9 and 12.3 for DMAPD and DEAPD, respectively. The smaller pyramidalization in DEAPD allows for a larger coupling between the amino and n_N in-ring orbitals, giving place to a larger oscillator strength value for the CT state in DEAPD of 0.39 and for DMAPD of 0.33, to be compared with 0.27 and 0.19 for DMA5MPD and APD, respectively. It also can have some effects in the kinetics of CT formation [32].

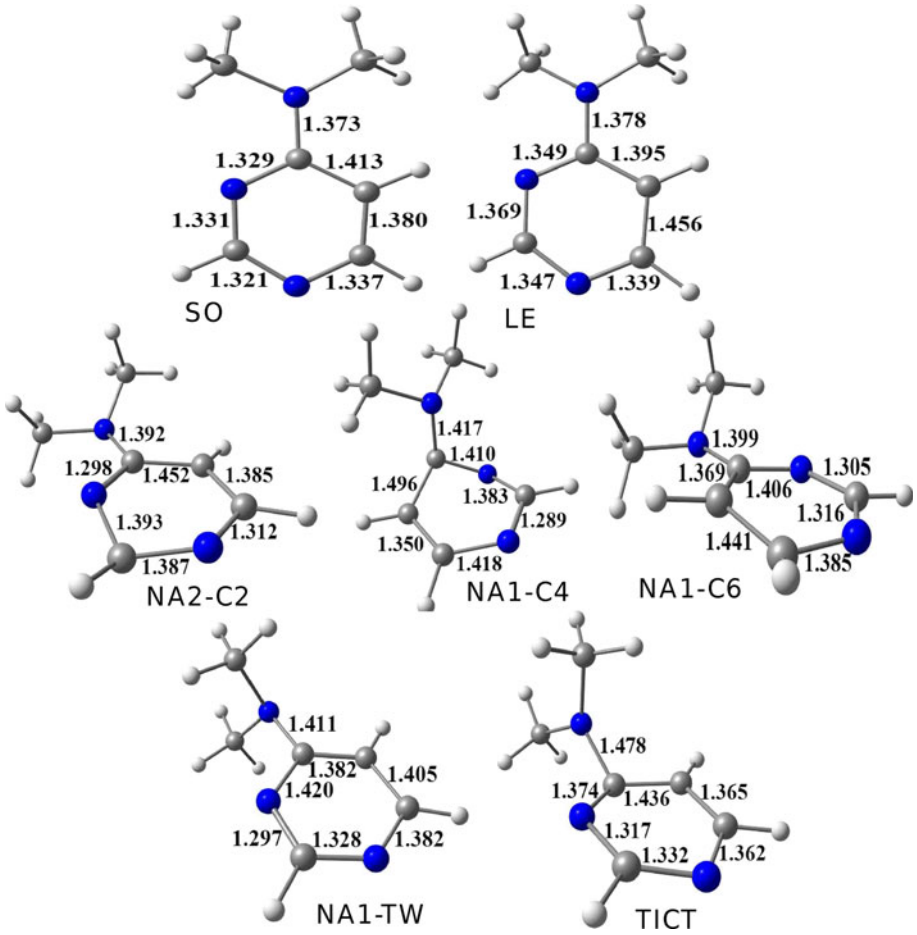

Fig. 4 Optimized structure of the S_0 minimum and S_1 intermediates of DMAPD

Table 3 Vertical excitation energies (in kcal mol^{-1}) and corresponding dipole moments and oscillator strengths of the substituted aminopyrimidines DMAPD, DMA5MPD and DEAPD calculated at the MS-CASPT2(12,11) level in gas phase

State Char.	DMAPD			DMA5MPD			DEAPD		
	ΔE	Dipole	Oscillator strength	ΔE	Dipole	Oscillator strength	ΔE	Dipole	Oscillator strength
LE	109.8	3.94	0.0129	99.1	4.29	0.0460	113.3	4.66	0.0692
NA1	116.8	2.02	0.0214	113.4	1.49	0.0115	121.8	2.35	0.0041
NA2	124.7	1.96	0.0226	128.9	2.69	0.0080	132.4	1.96	0.0167
CT	132.4	7.22	0.3383	133.0	6.80	0.2715	136.5	7.57	0.3900
NS1	150.0	1.52	0.0041	150.9	2.26	0.0244	159.8	1.95	0.0032
NS2	158.9	2.64	0.0062	–	–	–	–	–	–
CT2	–	–	–	–	–	–	163.5	6.44	0.0636
LE2	–	–	–	152.8	5.36	0.0911	–	–	–

Next, the Franck–Condon spectrum was calculated for all the substituted aminopyrimidines. The energetic ordering of the different excited states (Table 3) is basically the same than that found for APD at the MS-CASPT2 level, except for the LE and NA1 states, which swap their relative position, the LE state becoming the first excited state. However, there is an important lowering of the energy of the LE and CT states in the substituted analogs with respect to the unsubstituted APD. Actually, the CT stabilization is already seen in the absence of dynamic correlation, since it is already the fourth excited state at the CASSCF level (see data in the Supporting Information). The NA states remain practically at the same energy in all the molecules studied, except for DEAPD, where they are shifted to higher energies, together with the NS states, which are not found among the lowest six excited states. In all the cases, the

Table 4 Relative MS-CASPT2 energies to the S_0 minimum (ΔE), vertical energies (both in kcal mol^{-1}), dipole moments (in Debye) and oscillator strengths of the characterized S_1 minima for DMAPD

Minimum	ΔE	Vertical energy	Dipole moment	Oscillator strength
LE	100.7	95.5	4.91	0.0602
NA2	102.4	69.2	1.50	0.0015
NA1–C6	103.8	78.0	1.32	0.0057
NA1–C4	109.9	34.3	2.30	0.0001
NA1–TW	104.8	81.6	0.55	0.0070
TICT	97.4	54.6	7.02	0.0009

value of the oscillator strength shows that the CT state is likely to absorb most of the irradiated light, as found for APD. However, for substituted aminopyrimidines, the CT lies at lower energy than for the small APD already in the Franck–Condon region, and consequently, the CT is expected to be more accessible. For this reason, TICT formation has been explored in more detail for DMAPD and DM5MPD, to try to explain their luminescent behavior in gas phase and in a polar solvent.

Like for APD, we looked for the minima of the lowest excited states.

Regarding the DMAPD, the four lowest excited states were optimized and their minima located on the S_1 PES. Their energies relative to the ground state minimum are collected in Table 4 and their geometries shown in Fig. 4. The energetic data show that while the NA minima have about the same energy than in the APD analogs, the LE and CT intermediates undergo an important stabilization, which turn them into the most stable intermediates on the S_1 surface. This fact is consistent with the stabilization observed in the Franck–Condon region. In the LE minimum of this molecule, the out-of-ring amino group is not piramidalized, in contrast with the LE geometry found for APD, due to the donor ability of the alkyl substituents of DMAPD. There is also an increase in its dipole moment (4.91 D) with respect to the value for APD (3.56 D).

Given that the CT minimum is more stable than the LE one, but at the Franck–Condon region, these states are inverted, and there must be a crossing of the corresponding PES. This crossing would open a channel connecting these two lowest minima of the S_1 surface, of almost the same energy, and equilibrate their populations. To analyze this channel, we look for a conical intersection. The minimum energy point is located at 104.5 kcal mol^{-1} at CASSCF level above the ground state minimum. However, at this level of calculation, there is a mixing of the three N lone pair orbitals that preclude a clear determination of the nature of the states involved in the crossing. Moreover, when the dynamical correlation was included in the energy

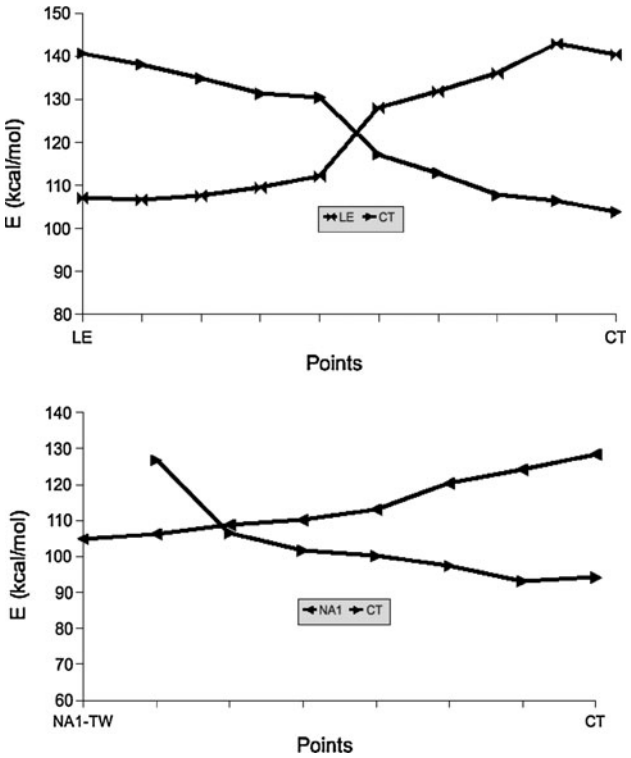

Fig. 5 Computed MS-CASPT2(12,11) LE–CT (*up*) and NA1–TW–CT (*down*) paths for DMAPD. Energies in kcal mol^{-1}

calculation, the states were not degenerated any longer. For this reason, a LIIRC path between the LE and CT minima was obtained, and the energy for the CT and the LE states was calculated along this path. The energy profiles obtained are shown in Fig. 5 (up). The height of the crossing point relative to the minima is not negligible, but the LE minimum can be populated when the conical intersection is reached in the relaxation path of the CT state from the Franck–Condon region. A latter equilibrium can be established between both minima if the system conserves the excess of excitation energy. To corroborate these hypotheses, dynamics calculations should be run, but they are out of the scope of this work.

The NA1–TW minimum has a geometry quite close to that of the CT minimum, reason why we investigated the possible population of the NA1–TW minimum from the CT one. Hence, a LIIRC path was built between these two minima, and the energies were calculated at the MS-CASPT2 level. The profiles represented in Fig. 5 (down) show that the barrier is almost negligible relative to the NA1–TW minimum, but the energy difference between minima will displace the equilibrium towards the CT species.

These results indicate that the favored minima on the S_1 surface will be the LE and CT ones. For APD, conical intersections of the excited states with the ground state were located only for NA states. Assuming that the same

Table 5 Relative MS-CASPT2 energies to the S_0 minimum (ΔE), vertical energies (both in kcal mol^{-1}), dipole moments (in Debye) and oscillator strengths of the characterized S_1 minima for DM5MADP

Minimum	ΔE	Vertical energy	Dipole moment	Oscillator strength
LE	107.0	99.1	4.61	0.0503
NA2	107.1	76.1	1.60	0.0007
NA1–C6	109.0	89.7	1.13	0.0089
NA1–C4	115.9	89.5	2.00	0.0102
NA1–TW	104.0	83.5	0.44	0.0088
NA2–TW	109.8	69.3	0.45	0.0008
NA1–C4–TW	108.2	60.5	1.67	0.0054
TICT	105.4	68.6	6.94	0.0054

feature holds for DMAPD, there is not accessible non-radiative deactivation paths for DMAPD, and luminescence becomes the only possible deactivation channel. Although both LE and CT minima can be populated, the oscillator strength for the transition to the ground state calculated for the CT state (0.0009) is two orders of magnitude smaller than that of the LE state (0.0602). Consequently, the thermodynamical equilibrium has to be highly favorable towards the TICT minima, in order to populate it for a large lifetime and allow the ICT fluorescence emission. In fact, the same would happen with the other NA and NS minima: even if they were populated, given that their oscillator strengths are also very small, radiative transition to the ground state would not take place. This explains the fact that the DMAPD only shows the normal fluorescence band in gas phase.

Turning now to the DM5MAPD, we looked for the most relevant S_1 minima and explored the ICT mechanism in the same way we did for DMAPD. The energetics of the minima is collected in Table 5, and the geometries were show in Fig. 6. In DM5MAPD, the CT minimum is stabilized with respect to the non-substituted APD, probably due to the donor effect of the alkyl substituents in the amino group. However, the LE minimum is less stabilized than for DMAPD, likely because of its planar nature, which forces the methyl substituent in the *ortho* position and the dimethylamino groups to be close and then destabilize the molecule. Related to this, the lowering of the unfavorable steric interaction between the substituents probably contributes to stabilize the new twisted NA1 and NA2 S_1 minima found, which are about 3–8 kcal mol^{-1} more stable than their planar analogs.

Regarding the paths connecting the S_1 minima, the CT–LE and CT–NA1–TW LIIRC's paths were also obtained for DM5MAPD. The energetic profiles obtained are shown in Fig. 7. The global characteristics are almost the same that those found for DMAPD, but in this case, the NA1–TW is almost isoenergetic with the CT minima and, given that the barrier connecting them is small, both minima can be equally populated. Nevertheless, in DM5AMPD, we found again that the oscillator strength for the transition to the ground state is much larger for the LE state (although in

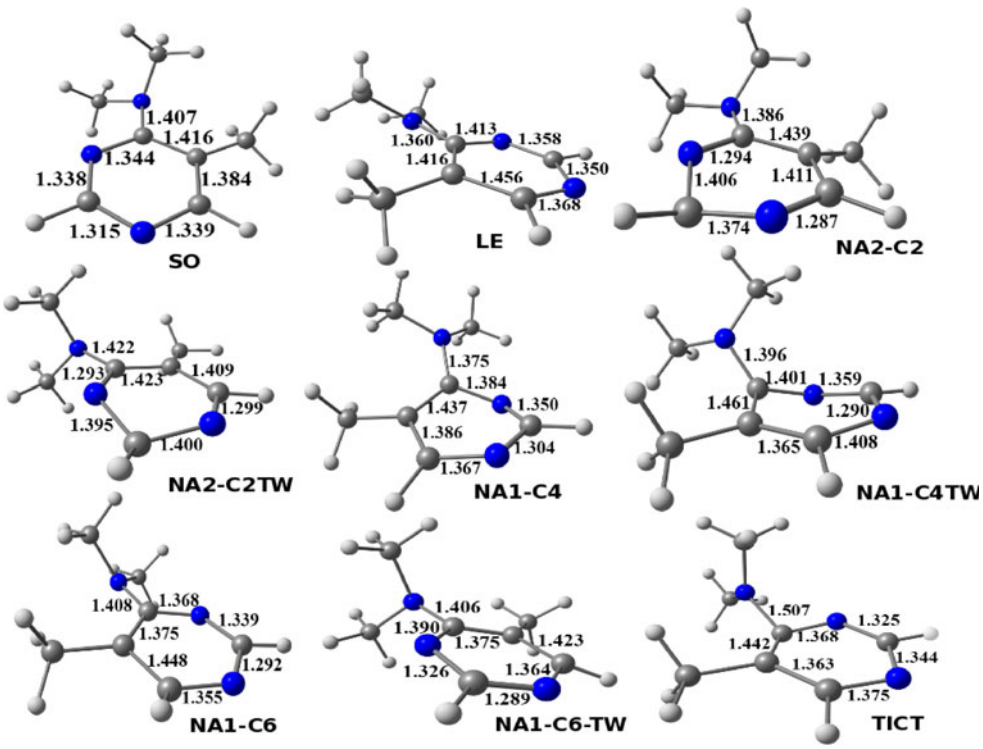

Fig. 6 Optimized structure of the S_0 minimum and the main S_1 intermediates of DMA5MPD

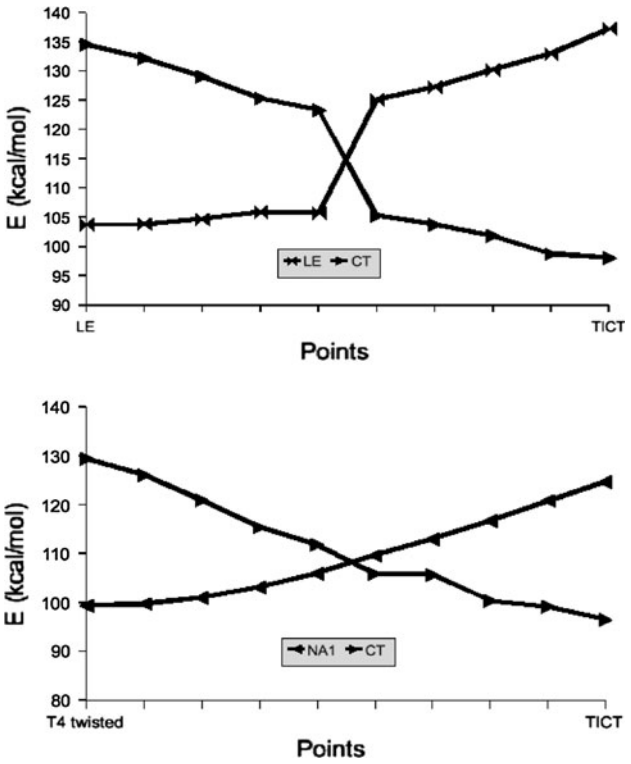

Fig. 7 Computed MS-CASPT2(12,11) LE–CT (*up*) and NA1–TW–CT (*down*) paths for DMA5MPD. Energies in kcal mol^{-1}

this case only one order of magnitude larger) that those of the CT and NA1–TW states, for the same reasons exposed for DMAPD. Consequently, also in this case the luminescent deactivation will take place only from the LE minimum, and the NA1–TW and TICT states will be depopulated trying to keep the equilibrium with the LE state.

As we already commented in the introduction, DMAPD shows only normal fluorescence in gas phase and in polar aprotic solvents, while DMA5MPD shows only normal fluorescence in gas phase but only anomalous fluorescence in polar aprotic solvents. Due to this interesting difference, and trying to explain it, we have also studied the effect of a polar aprotic solvent (acetonitrile) on the S_1 PES of these two APD derivatives by means of the PCM model. Results are summarized in Table 6 and show that in both cases the environment stabilizes the TICT and LE minima (their energies relative to the S_0 minimum are 89.0 and 90.8 kcal mol^1 for DMAPD and 86.0 and 100.0 kcal mol^{-1} for DMA5MPD) and slightly destabilizes the NA1 and NA2 states, probably due to its low dipolar moment. Consequently, the most stable S_1 minima in a polar solvent are the LE and CT minima, so these minima will be populated preferentially.

In gas phase, the small energetic difference between the LE and TICT minima (about 3.3 and 1.6 kcal mol^{-1} in DMAPD and DM5MAPD, respectively) did not

Table 6 Relative MS-CASPT2-PCM energies to the S_0 minimum (ΔE) and vertical energies (both in kcal mol^{-1}) of the characterized S_1 minima for DMAPD and DMA5MDP in acetonitrile

State	DMAPD	DMA5MDP
LE	90.8	102.5
NA2	98.8	107.7
NA1–C6	100.6	114.4
NA1–TW	–[a]	108.7
NA2–TW	–	
NA1–C4–TW	–	111.8
TICT	89.0	85.0

[a] The first excited state at the NA1–TW geometry shows CT character when solvent is considered

compensate the difference in the magnitude of the oscillator strength for the radiative transition to the ground state so only emission from the LE minimum was observed in both case. In a polar solvent, this situation does not change for DMAPD, because the energy difference between the LE and TCT minima continues being very small (1.8 kcal mol^{-1}), so again only the normal fluorescence band is expected (in agreement with experimental results). But for DMA5MPD, the situation in acetonitrile is different, because the TICT minimum is strongly stabilized, becoming 17.5 kcal mol^{-1} more stable than the LE minimum. In this case, the thermodynamical equilibrium is well displaced towards the TICT minimum, and in spite of the lower oscillator strength for the transition to the ground state, the TICT can emit being the ICT band the only one observed.

Globally, the luminescence pattern seems to be governed by the energy difference between the LE and CT minima. At this point, it is interesting to corroborate this hypothesis with DEAPD, which shows only the normal band in the gas phase but dual fluorescence in polar environments. For DEAPD, we have located the LE and CT minima on the S_1 surface and calculated their energies in gas phase and in acetonitrile. Geometries are shown in Fig. 8 and energies in Table 7. In gas phase, the CT minimum is only 4 kcal mol^{-1} more stable than the LE one, an energy difference similar to the ones found for DMAPD and DMA5MPD in gas phase so, like in those cases, only the normal band is observed also for DEAPD. In acetonitrile, this difference increases up to 9.9 kcal mol^{-1}, which is smaller than the one found for DMA5MPD but larger than that of DMAPD. It can be due to the donor effect of the diethyl group that stabilizes the CT minimum more than the methyl groups do in DMAPD, and to the lack of steric effects of the C_5 substituent that destabilizes the LE species in DM5MAPD. This effect also affects the dipole moment, higher for the diethyl-substituted molecule. As a result, the equilibrium in DEAPD is only partially

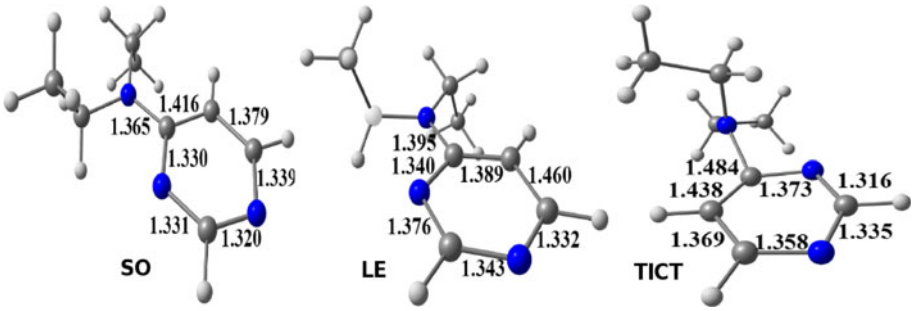

Fig. 8 Optimized structure of the S_0 minimum and the main S_1 DEAPD intermediates

Table 7 MS-CASPT2(12,11) relative energies (in kcal mol^{-1}), dipole moments (in Debye) and oscillator strengths of the LE and CT minima for DEAPD, calculated both in gas phase and in acetonitrile

Minimum	ΔE	Vertical energy	Dipole moment	Oscillator strength	$\Delta E_{solvent}$
LE	105.9	97.5	4.95	0.0558	0.0
CT	101.3	62.7	7.78	0.0007	−9.9

displaced towards the CT minimum, keeping the LE minimum also partially populated. The larger oscillator strength of the transition to the GS from the LE allows this species to emit, in spite of its smaller population, and the larger population of the TICT minimum allows this other species also to emit, in spite of its smaller oscillator strength. The dual fluorescence observed for DEAPD in polar solvents is in this way explained.

4 Conclusions

In this work, we have studied the photochemistry of the APD and three derivatives to elucidate the factors that determine the luminescent properties of this family of compounds and how the substituents affect it. To do so, we have studied first in more extension the excited states of the parent system, the APD, to determine the factors that are crucial in the photochemical processes that lead to final deactivation of the system after photoexcitation. In a second step, we have analyzed these factors for the DMAPD, DEAPD and DMA5MPD derivatives looking for the differences that explain the different luminescent behavior. Finally, we have taken into account the effect of a polar solvent to understand how this environmental change affects the luminescent of these compounds.

In the study developed for the parent system, APD, the results show that the photochemistry is determined by the relative stability of the minima on the S_1 PES of the different types of excited states and the paths connecting them. The substituents of the derivative systems affect the relative stability of these minima. First of all, the alkyl substituents of the amino group stabilize preferentially the LE and CT excited states of the system. This is the due to donor effect of the alkyl substituents, which also reduce the pyramidalization of the amino group. In fact, for the unsubstituted APD, the amine is pyramidalized, while for the rest the structure of the LE, minima is nearly planar. In addition, when there is a bulky substituent in the *ortho* position, the steric repulsion between the substituents destabilizes the planar LE minimum, favoring the CT excited state.

Regarding the luminescent behavior, if the NA minima on S_1 are more stable than the LE and CT ones, the most effective reactive channel is the non-radiative deactivation through the very accessible conical intersections that exist between the NA excited states and the ground state. In this case, p.e. for APD, luminescent will not be observed.

On the other hand, if the CT and LE minima on the S_1 surface are more stable than the NA minima, the non-radiative deactivation channels are not accessible, and the deactivation of the system occurs necessarily through emission. The radiative species is determined by two factors: the relative stability of the LE/CT minima and the value of the oscillator strength for the radiative transition to the ground state. Given that this oscillator strength is much larger for the LE state than for the CT one, the CT minima must be much more stable than the LE one to be competitive in the radiative deactivation reaction.

For the three derivatives DMAPD, DMA5MPD and DEAPD in gas phase, the NA minima are less stable than the LE and CT ones, being the last two almost isoenergetics (CT–LE energy differences: 3.4, 1.6 and 4.6 kcal mol^{-1}, respectively). This leads to a common luminescent pattern, where only the normal fluorescence band is observed.

Polar solvents stabilize preferentially the CT minimum relative to the LE one, and the size of this relative stabilization depends partially on the magnitude of the dipole moment of both species in the different compounds.

As a whole, the stabilization is larger for the DMA5MPD, where ΔE_{CT-LE} is 17.5 kcal mol^{-1}. This difference is large enough to lead to luminescence exclusively from the CT minima. Consequently, for this compound, only the anomalous fluorescence band is observed in polar solvents. The DEAPD is the intermediate case, where the ΔE_{CT-LE} is only of 9.9 kcal mol^{-1}. In this case, both radiative deactivations are competitive and dual fluorescence is observed in polar solvents. For DMAPD, the ΔE_{CT-LE} is only 1.8 kcal mol^{-1} so, like in gas phase, only the normal fluorescence band is observed.

The good agreement between the computational results and the experimental observations support the hypothesis proposed in this work, where the luminescent behavior of several members of the aminopyrimidine family is justified.

Acknowledgments This work was supported by Generalitat de Catalunya (SGR2009-462), Spanish Ministerio de Ciencia e Innovación (CQT-2008-06644-C02-01) and MAC Juan de la Cierva grant.

References

1. Lagoja IM (2005) Chem Biodivers 2:1–50
2. Schellenberger A, Hubner G, Neef H (1997) Methods Enzymol 278:131–146
3. Mrowca JJ (1996) 5523405
4. Roth B, Cheng CC (1982) Prog Med Chem 19:268–330
5. El-Ghayoury A, Schenning APHJ, Van Hal PA, Van Duren JKJ, Janssen RAJ, Meijer EW (2001) Angew Chem 113:3772–3775
6. El-Ghayoury A, Schenning APHJ, Van Hal PA, Van Duren JKJ, Janssen RAJ, Meijer EW (2001) Angew Chem Int Ed 40:3660–3663
7. Kim YJ, Kim JH, Kang MS, Lee MJ, Won J, Lee JCh, Kang YS (2004) Adv Mater 16:1753–1757
8. Huang Ch H, McClenaghan ND, Kuhn A, Bravic G, Bassani DM (2006) Tetrahedron 62:2050–2059
9. Hegmann T, Kain J, Diele S, Schubert B, Bögel H, Tschierske C (2003) J Mater Chem 13:991–1003
10. Grabowski ZR, Rotkiewicz K, Siemiarczuk A, Cowley DJ, Baumann W (1979) Nouv J Chim 3:443–454
11. Grabowski ZR, Rotkiewicz K, Rettig W (2003) Chem Rev 103:3899–4032
12. Calza P, Medana C, Baiocchi C, Pelizzetti E (2004) Appl Catal B: Environ 52:267–274
13. Hoffman JE, Cheng H, Rheingold AL, DiPasquale A, Yanovsky A (2009) Acta Cryst E 65:02374
14. Li C, Rosenau A (2009) Tetrahedron Lett 50:5888–5893
15. Herbich J, Grabowski ZR, Wojtowicz H, Golankiewicz K (1989) J Phys Chem 93:3439–3444
16. Herbich J, Salgado FP, Rettschnick RPH, Grabowski ZR, Wójtowicz H (1991) J Phys Chem 95:3491–3497
17. Rettig W (1986) Angew Chem Int Ed Engl 25:971–988
18. Cogan S, Zilberg S, Haas Y (2006) J Am Chem Soc 128:3335–3345
19. Zechmann G, Barbatti M (2008) Int J Quantum Chem 108:1266–1276
20. Barbatti M, Ruckenbauer M, Szymczak JJ, Aquino AJA, Lischa H (2008) Phys Chem Chem Phys 10:482–494
21. Hariharan PC, Pople JA (1973) Theor Chim Acta 28:213–222
22. Karlström G, Lindh R, Malmqvist PÅ, Roos BO, Ryde U, Veryazov V, Widmark PO, Cossi M, Schimmelpfennig B, Neograd y P, Seijo L (2003) Comput Mater Sci 28:222–239
23. Frisch MJ, Trucks GW, Schlegel HB, Scuseria GE, Robb MA, Cheeseman JR, Montgomery JA Jr, Vreven T, Kudin KN, Burant JC, Millam JM, Iyengar SS, Tomasi J, Barone V, Mennucci B, Cossi M, Scalmani G, Rega N, Petersson GA, Nakatsuji H, Hada M, Ehara M, Toyota K, Fukuda R, Hasegawa J, Ishida M, Nakajima T, Honda Y, Kitao O, Nakai H, Klene M, Li X, Knox JE, Hratchian HP, Cross JB, Bakken V, Adamo C, Jaramillo J, Gomperts R, Stratmann RE, Yazyev O, Austin AJ, Cammi R, Pomelli C, Ochterski JW, Ayala PY, Morokuma K, Voth GA, Salvador P, Dannenberg JJ, Zakrzewski VG, Dapprich S, Daniels AD, Strain MC, Farkas O, Malick DK, Rabuck AD, Raghavachari K, Foresman JB, Ortiz JV, Cui Q, Baboul AG, Clifford S, Cioslowski J, Stefanov BB, Liu G, Liashenko A, Piskorz P, Komaromi I, Martin RL, Fox DJ, Keith T, Al-Laham MA, Peng CY, Nanayakkara A, Challacombe M, Gill PMW, Johnson B, Chen W, Wong MW, Gonzalez C, Pople JA (2004) Gaussian 03, Revision C.02. Gaussian Inc, Wallingford
24. Angeli C (2009) J Comput Chem 30:1319–1333
25. Angeli C (2010) Int J Quantum Chem. doi:10.1002/qua.22597
26. Malmqvist PÅ, Roos BO, Fülscher MP, Rendell AP (1992) Chem Phys 162:359–367
27. Barone V, Cossi M (1998) J Phys Chem A 102:1995–2001
28. Cossi M, Rega N, Scalmani G, Barone V (2001) J Chem Phys 114:5691–5701
29. Tomasi J, Mennucci B, Cammi R (2005) Chem Rev 105:2999–3093
30. Gomez I, Reguero M, Boggio-Pasqua M, Robb MA (2005) J Am Chem Soc 127:7119–7129
31. Gomez I, Mercier Y, Reguero M (2006) J Phys Chem A 110:11455–11461
32. Zachariasse KA, Grobys M, Von der Haar T, Hebecker A, Il'ichev YV, Jiang YB, Morawski O, Kühnle W (1996) J Photochem Photobiol A: Chem 102:59–70